Tetrahedron 64 (2008) 5598–5603

Contents lists available at ScienceDirect

Tetrahedron

journal homepage: www.elsevier.com/locate/tet

Conformational probe: static quenching is reduced upon acid triggered ring flip of a *myo*-inositol derivative

Manikandan Kadirvel, Abdul Gbaj, David Mansell, Steven M. Miles, Biljana Arsic, Elena V. Bichenkova *, Sally Freeman *

School of Pharmacy and Pharmaceutical Sciences, University of Manchester, Oxford Road, Manchester M13 9PT, United Kingdom

ARTICLE INFO

Article history:
Received 21 December 2007
Received in revised form 3 March 2008
Accepted 13 March 2008
Available online 15 March 2008

Keywords:
Excimer
Exciplex
Fluorescent probe
Trigger
Inositol
Conformation
Static quenching

ABSTRACT

The aromatic rings in 4-*O*-dabsyl-6-*O*-dansyl-*myo*-inositol-1,3,5-orthoformate (**6**) participate in electron transfer causing static quenching as detected by the absence of fluorescence. Upon addition of acid, the orthoformate lock is cleaved, with subsequent conformational change of the *myo*-inositol ring from penta-axial to the more stable penta-equatorial chair, which causes some increase in fluorescence due to spatial separation of fluorophore and a quencher and reduction in static quenching. In the case of 4,6-*O*-bisdansyl-*myo*-inositol-1,3,5-orthoformate (**3**), the acid-induced removal of the orthoformate lock leads to substantial change of fluorescence following spatial separation of two dansyl groups.

1. Introduction

Fluorescent molecular probes have been designed to monitor some important biochemical events, detect complex bio-molecular assemblies[1–3] and identify specific tissues or organelles with unique physiological or pathological functions.[4] Fluorescent molecules conjugated with carbohydrates have been studied extensively in the field of molecular imaging as a safe alternative to radioactive probes.[5–8] We have introduced recently the first exciplex-based oligonucleotide split probes that can self-assemble at their complementary DNA target to produce emissive exciplexes with their characteristic long-wavelength fluorescence.[1,2] This method can efficiently detect single mutations and, thus, represents a new approach for genotyping and gene expression profiling. Our next challenge is to develop novel molecular devices capable of detecting and signalling the presence of certain chemical or biological factors (e.g., high cellular levels of H^+, metal ions or certain enzymes) via inositol conformational flip triggered by these factors. We have recently reported our pilot studies[9] on acid-induced conformational flip of the 1,3,5-orthoformate and 1,3,5-orthoacetate *myo*-inositol derivatives **1** and **2**, monitored by the disappearance of excimer and exciplex fluorescence, respectively. Orthoformate protection of *myo*-inositol is routinely used, in contrast to protection of triols in carbohydrates.[10] The scope of this study can be extended as $Pd(OH)_2/C$, MeMgBr and DIBAL-induced deprotection of orthoformate inositol esters have also been reported.[11–13] Esters **1** and **2** adopt unstable chair conformations with five substituents in axial positions, in which the aromatic esters participate in π-stacking, and give green fluorescence at ~520 nm. Upon addition of acid, the orthoformate/orthoacetate lock is cleaved, which allows the *myo*-inositol ring to switch to the more stable penta-equatorial chair conformation, with a loss of exciplex/excimer green fluorescence.[9] Disappearance of exciplex or excimer signal was accompanied by the appearance of a locally excited state (LES) band at around 380 nm producing blue fluorescence and, thus, resulting in the visual fluorescent colour change. This characteristic colour signalling of exciplex/excimer probes means that direct visualisation approaches are possible for detection of conformational rearrangements. An alternative to the above concept would be a replacement of exci-partners with a suitable *fluorophore–quencher* couple. In this approach, emission of the fluorescent moiety is quenched by resonance energy transfer from fluorophore (fluorescence energy donor) to quencher (energy acceptor) via non-radiative transfer of excitation energy. Dynamic quenching occurs when the donor is in its *excited state* and proceeds either via Förster or Dexter mechanism.[14] Static quenching[14–16] occurs as a result of

* Corresponding authors. Tel.: +44 161 275 2401; fax: +44 161 275 2396 (E.V.B.); tel.: +44 161 275 2366; fax: +44 161 275 2396 (S.F.).
E-mail addresses: elena.v.bichenkova@manchester.ac.uk (E.V. Bichenkova), sally.freeman@manchester.ac.uk (S. Freeman).

0040-4020/$ – see front matter © 2008 Elsevier Ltd. All rights reserved.
doi:10.1016/j.tet.2008.03.045

interactions between fluorophore and quencher at their *ground state*, leading to formation of a ground-state complex (an intramolecular heterodimer) with its own unique absorption and fluorescence properties. As an improvement to the *fluorophore–quencher* concept, an acceptor molecule has recently been replaced with a *dark quencher* (dye molecule with no native fluorescence) to avoid the fluorescence background noise of the acceptor.[17,18] Another strategy is the use of two identical dyes to produce ground-state intramolecular homodimers with substantially different fluorescence,[14] when the dyes are closely located in space.

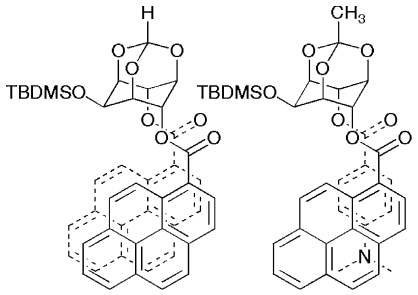

In this research, we report on the application of the fluorescence-based strategy to detect the conformational flip of inositol-based molecular probes via formation of ground-state hetero- and homodimers. We demonstrate here that acid-induced removal of the orthoformate lock leads to a change of fluorescence as a response to the inositol conformational flip and subsequent spatial separation of reporter groups.

2. Results and discussion

To observe the conformational flip of the inositol ring with a change of fluorescence, intramolecular homodimer **3** and heterodimer **6** have been designed by conjugation of dansyl and dabsyl groups to the 4- and 6-position of *myo*-inositol-1,3,5-orthoformate via sulfonate esters (Scheme 1).

Compounds **3** and **6** show the dansyl and dabsyl groups in their possible π-stacked conformations. The 2-silylated intermediate **4** was prepared by treating *myo*-inositol with triethyl orthoformate followed by the regiospecific protection of the 2-equatorial hydroxyl group.[19,20] The homodimer **3** was prepared in 72% yield by sulfonation[21] of the 4,6-diaxial hydroxyl groups using dansyl chloride[22] in the presence of sodium hydride. Some of the monomer **5** was also formed. The heterodimer **6** was prepared in 45% yield by treating the intermediate **4** with 6 equiv sodium hydride followed by an equivalent of dabsyl chloride.[9] After 10 min, addition of dansyl chloride led to the formation of the mixed ester **6** together with some monomer **7** (Scheme 1). Dimers **3** and **6** were isolated after purification by flash column chromatography and were fully characterised by NMR spectroscopy, mass spectrometry and elemental analysis.

These dimers should give changes in UV–visible absorption and fluorescence emission spectra when the chair conformation of intramolecular dimers is flipped. The orthoformate deprotection of esters **3** and **6** was achieved by treatment with 80% trifluoroacetic acid.[11] Deprotection of homodimer **3** was clean giving rise to only open bisdansyl dimer **8**, isolated in 75% yield (Scheme 2). In contrast, the deprotection of heterodimer **6** was more complex giving rise to the expected open analogue of mixed ester **9**, together with open dansyl monomer **10**, arising from dabsyl sulfonate ester hydrolysis (Scheme 3).

UV–visible and fluorescent spectroscopic studies of compounds **3** and **5**–**10** were performed at 2 μM concentrations to minimise any intermolecular interactions. The fluorescence intensities of

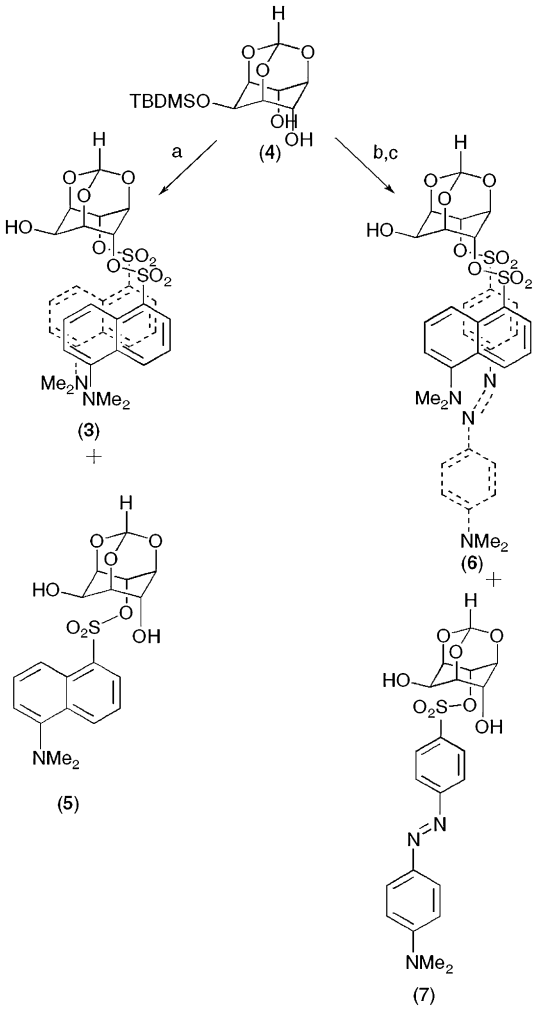

Scheme 1. Synthesis of 4,6-diaxial sulfonates **3**, **5**, **6** and **7**: (a) dansyl chloride, 60% sodium hydride, dry DMF; (b) dabsyl chloride, 60% sodium hydride, dry DMF; (c) dansyl chloride.

dual-labelled probes **3** and **6**, measured over a range of concentrations, showed a linear relationship between fluorescence intensity and concentration for the region between 1 and 6 μM (data not shown). This ensured that the spectral changes observed under experimental conditions (2 μM) for **3** and **6** were attributed to intramolecular interactions rather than intermolecular aggregation in aqueous solutions.

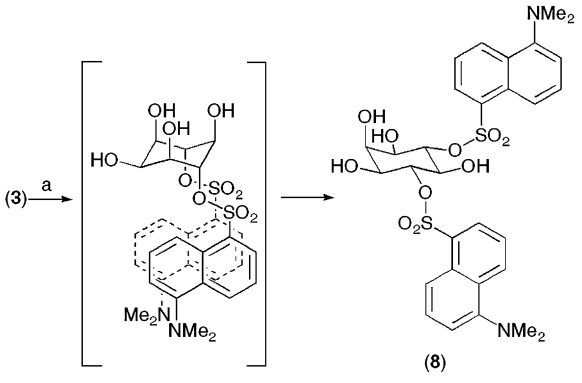

Scheme 2. Acid hydrolysis of 4,6-bis-*O*-dansyl-*myo*-inositol-1,3,5-orthoformate **3**: (a) 80% trifluoroacetic acid.

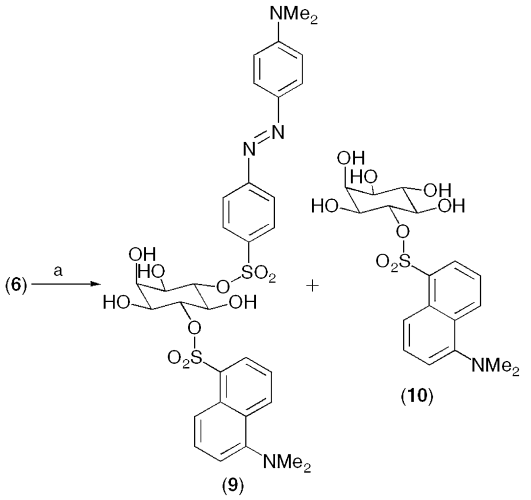

Scheme 3. Acid hydrolysis of 4-*O*-dabsyl-6-*O*-dansyl-*myo*-inositol-1,3,5-orthoformate **6**: (a) 80% trifluoroacetic acid.

The UV–visible spectrum of a singly labelled 4-*O*-dansyl monomer **5** showed an absorption band at 334 nm (Fig. 1A). Singly labelled probe **7** containing the 4-*O*-dabsyl quenching group displayed a broad absorption band with two maxima at ~390 nm and ~480 nm. The dual-labelled probe **6** containing both 6-*O*-dansyl fluorophore and 4-*O*-dabsyl quencher displayed a rather broad, intensive and structure-less absorption band between 360 and 560 nm, which substantially differed from the UV–visible characteristics of individual monomer probes **5** and **7**. The shoulder observed at 380 nm for **6** was markedly distorted and blue-shifted by approximately 10 nm as compared with the corresponding absorption band of **7** seen at 390 nm. The absorption band of the dansyl component was also blue-shifted and not clearly resolved for **6**. It is seen from Figure 1A that the UV–visible spectrum of **6** cannot be reconstructed by summing of the absorption spectra of the singly labelled probes **5** and **7** and, thus, is not merely additive. These observations indicate intramolecular interaction between 6-*O*-dansyl fluorophore and 4-*O*-dabsyl quencher in **6** at their ground state leading to the formation of an intramolecular heterodimer with its unique UV–visible characteristics (Fig. 1A).

The fluorescent spectrum of the singly labelled probe **5** showed an emission band at 600 nm following excitation at 335 nm. In contrast, only negligible fluorescence was observed in the emission spectrum of **6** under identical experimental conditions, indicating effective static quenching of 6-*O*-dansyl fluorophore by closely located 4-*O*-dabsyl quencher (Fig. 1B). As a result, fluorescence intensity of **6** was reduced by a factor of 35 as compared with that of dansyl monomer **5**. Significant quenching observed for **6** presumably occurred due to minimal overlap between the emission band of dansyl fluorophore and absorption band of dabsyl quencher, which is consistent with the static quenching seen for the ground-state heterodimers.[23]

Acid-induced removal of the orthoformate lock, leading to the formation of **9**, resulted in the anticipated conformational rearrangement of the inositol ring accompanied by spatial separation of 6-*O*-dansyl fluorophore and 4-*O*-dabsyl quencher. This inositol conformational flip was reflected by both UV–visible and fluorescence spectra of **9**. Compound **9** showed some level of restoration of UV–visible absorption bands of both dansyl and dabsyl components at 330 and 484 nm, respectively (Fig. 1A). The intensity of these absorption bands has not been fully recovered presumably due to effective fluorophore–quencher interactions (Fig. 1A). The fluorescence spectrum of **9** showed some increase of fluorescence emission and the fluorescence intensity of **9** was approximately three times higher than that of **6** (Fig. 1B). These data demonstrate that the conformational flip separates fluorophore and quencher in **9** leading to a slight increase in fluorescence. However, the quenching of fluorescence is still observed, presumably due to the fact that the fluorophore and quencher still interact with each other in the open structure **9**. These results are in agreement with our molecular modelling data obtained using molecular dynamics. The computer calculations of **6** revealed that its most stable low energy conformation (E=9.1 kcal/mol) corresponds to the structure with almost parallel orientation and π–π-stacking interactions between the aromatic rings of dabsyl and dansyl groups (Fig. 2). The distance between molecular centroids of fluorophore and quencher was found to be 3.6 Å, which explains a very efficient quenching of fluorescence, observed experimentally. Compound **9** shows a high level of conformational flexibility. We found a number of low energy conformations with the centroid distance between dansyl and dabsyl groups ranging from 5.1 Å to 12.9 Å. One example of a low energy conformation of **9** (E=21.1 kcal/mol) with the distance between fluorophore and quencher centroids of 12.9 Å is shown in Figure 2. These observations confirm that the fluorescence of dansyl groups by dabsyl quencher could be very efficient even in the open conformation of **9**, presumably due to the high population of conformations with closely located fluorophore and quencher. These observations revealed that the energy transfer mechanism is quite effective over large distances between the fluorophore and the quencher, which resulted in residual quenching of monomer fluorescence.[14]

The homodimer **3** also demonstrated formation of the ground-state intramolecular complex between two dansyl fluorophore: UV spectrum of **3** showed a substantial red shift in the dansyl

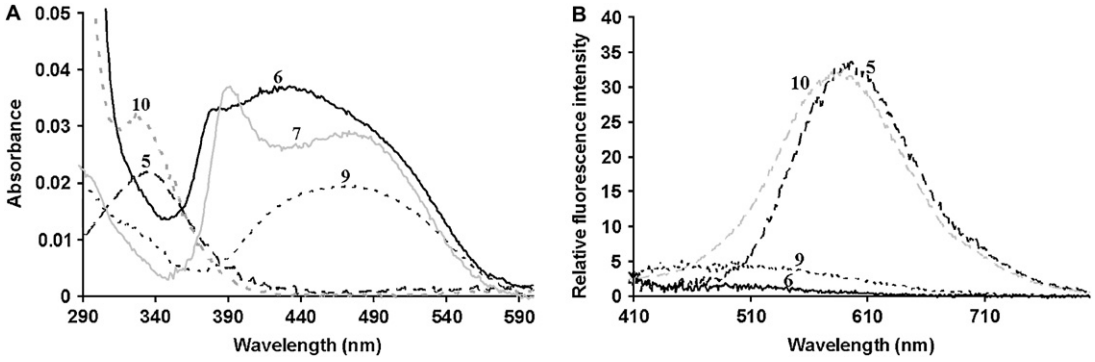

Figure 1. (A) UV and (B) fluorescence spectra of 4-*O*-dabsyl-6-*O*-dansyl-*myo*-inositol-1,3,5-orthoformate (**6**, —), 4-*O*-dabsyl-*myo*-inositol-1,3,5-orthoformate (**7**, —), 4-*O*-dansyl-*myo*-inositol-1,3,5-orthoformate (**5**, - -), 4-*O*-dabsyl-6-*O*-dansyl-*myo*-inositol (**9**, · ·) and 4-*O*-dansyl-*myo*-inositol (**10**, - -). Spectra were recorded at 2 μM concentration in pH 7.4 phosphate buffer at 20 °C. Excitation and emission slit widths were 10 nm and spectra are buffer corrected.

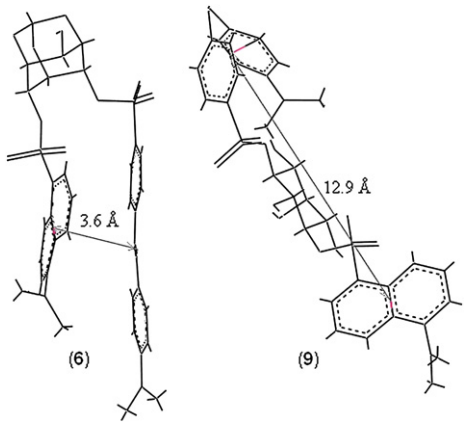

Figure 2. Energy minimised structures of **6** and **9** from SYBYL 7.3 (Tripos force field).

absorption band by approximately 40 nm (Fig. 3A) as compared with the singly labelled monomer **5**, presumably indicating strong π-stacking interactions of the naphthalene rings.[24] In addition, high intensity fluorescence emission was observed for **3** at 524 nm (Fig. 3B), which was blue-shifted as compared with the emission band of dansyl monomer **5** observed at ~600 nm. Acid-induced deprotection of **3**, leading to formation of **8**, resulted in substantial changes of both UV-absorption and emission spectra (Fig. 3A and B, respectively), indicating distortion of the ground-state dansyl homodimer. UV–visible absorption band of deprotected analogue **8** is shifted back to a shorter wavelength region giving an absorption band at ~330 nm. The emission spectrum of **8** showed complete loss of the characteristic J-aggregate band at 524 nm accompanied by the appearance of two emission bands at 455 and 584 nm, similar to those observed for the dansyl monomer **5**.

3. Conclusions

In summary, π–π-stacked *myo*-inositol 4,6-diester **6** does not fluoresce due to quenching of the donor and acceptor pairs. On conformational change, the ring flipped diester **9** is slightly fluorescent due to the absence of π–π-stacking, however, some quenching was still observed due to the close distance between the fluorophore and quencher (minimum ~5.1 Å, maximum ~12.9 Å) allowing residual energy transfer. In the case of 4,6-bis-*O*-dansyl-*myo*-inositol-1,3,5-orthoformate **3**, the deprotection of the orthoformate lock results in a substantial change of fluorescence, which signals conformational flip of the inositol ring. This study provides a possible way for the development of imaging probes for acidic compartments (e.g., vacuoles and hypoxic tumour cells).

4. Experimental

4.1. General methods

Chemicals were purchased from Aldrich Chemical Co., Gillingham, UK. Syntheses were monitored by thin layer chromatography on pre-coated 60 F_{254} silica gel aluminium backed plates (Merck, Darmstadt). Visualisation of spots for thin layer chromatography was performed using an UV GL-58 Mineral-Light lamp. Flash column grade 40–63 μm silica gel (Apollo scientific, Stockport, UK) was used in preparative scale column chromatography. Melting points were determined using a Gallenkamp Melting Point apparatus microscope (UK). IR spectra were recorded using a Bruker Tensor 27 spectrometer, resolution 4 cm^{-1}. NMR spectra were recorded using a Bruker Avance-300 spectrometer (7.05 T) equipped with a 5 mm single-axis *Z*-gradient quattro nucleus probe, operating at 300 MHz for ^{1}H and at 75 MHz for ^{13}C. The spectrometer was running TOPSPIN NMR system software (Version 2.0). Chemical shifts (δ) are reported in parts per million (ppm), peak positions relative to Me_4Si (0.00 ppm) for ^{1}H and ^{13}C NMR spectra. Abbreviations used for splitting patterns are: s, singlet; d, doublet; t, triplet; qt, quartet; pt, pentet; m, unresolved multiplet. Mass spectra were recorded at the Chemistry Department, University of Manchester using a Micromass PLATFORM II (ES) and Thermo Finnigan MAT95XP (Accurate mass) instrument.

Fluorescence emission and excitation spectra were recorded in 2 ml quartz thermostatted cuvettes using a controlled-temperature Cary-Eclipse fluorescence spectrophotometer. Emission and excitation spectra were recorded in phosphate buffer pH 7.4 (0.1 M). The excitation wavelength used was 335 nm. Slit widths were 10 nm. The automatic shutter-on function was used to minimise photo-bleaching of the sample. UV–visible spectra were recorded in 1 ml quartz cuvettes using a Cary 4000 UV–visible spectrophotometer equipped with a Peltier-thermostatted cuvette holder. The pH was measured using a Hanna-instruments HI 9321 microprocessor pH meter, calibrated with standard buffers (Sigma) at 20 °C.

The conformational search was performed in SYBYL 7.3[25] using Tripos force field[26] in water as the solvent (ε=80.4). The Gasteiger-Huckel charges were used throughout the calculations. Conformations of structures **6** and **9** were obtained from initial drawn structures minimised by Tripos force field[26] followed by simulated annealing (heated to 500 K for 2000 fs and then cooled to 0 K for 10,000 fs). The number of iterations for each constrained conformational search was 10,000 and the search was terminated

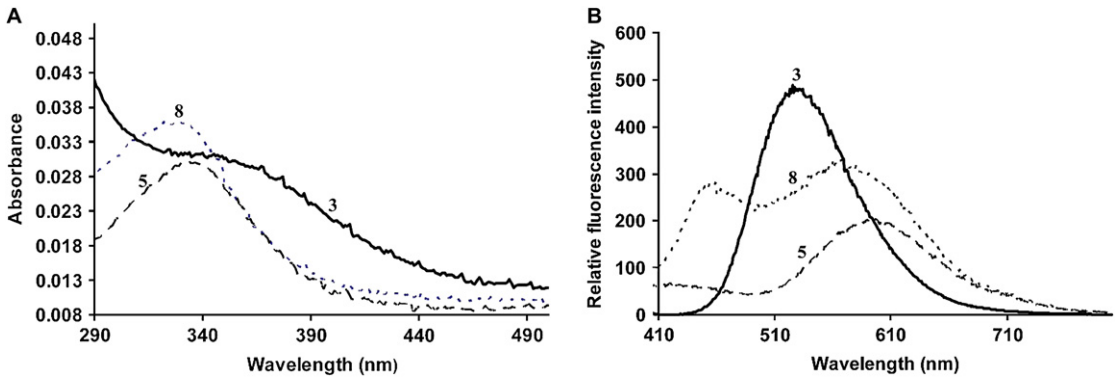

Figure 3. (A) UV and (B) fluorescence spectra of 4,6-bis-*O*-dansyl-*myo*-inositol-1,3,5-orthoformate (**3**, —), 4-*O*-dansyl-*myo*-inositol-1,3,5-orthoformate (**5**, - -) and 4,6-*O*-bisdansyl-*myo*-inositol (**8**, · ·). Spectra were recorded at 2 μM concentration in pH 7.4 phosphate buffer and 20 °C. Excitation and emission slit widths were 10 nm and spectra are buffer corrected. Fluorescence spectra of compounds **5** and **8** are multiplied by 6.

gradiently when the difference in energies between two conformations was no more than 0.005 kcal/mol.

4.2. Synthesis

4.2.1. 4,6-O-Bisdansyl-myo-inositol-1,3,5-orthoformate (3)

Sodium hydride (60%, 0.16 g, 3.9 mmol) was suspended in dry DMF (20 ml) and the mixture was stirred at room temperature under a nitrogen atmosphere. 2-*O*-*tert*-Butyldimethylsilyl-*myo*-inositol-1,3,5-orthoformate[20] **4** (0.3 g, 1.0 mmol) was added to the above solution and the mixture was stirred at room temperature for 10 min. Dansyl chloride (0.56 g, 2.1 mmol) was added under a nitrogen atmosphere and the mixture was stirred for a further 24 h. The reaction was monitored by TLC (DCM/ethyl acetate 3:1), R_f 0.74. The reaction mixture was carefully quenched with 0.01 M HCl (20 ml). The mixture was diluted with ethyl acetate (100 ml), the layers were separated and the organic layer was washed with water (6×25 ml). The organic layer was washed further with 10% $NaHCO_3$ (2×20 ml). The organic layer was dried over anhydrous magnesium sulfate, filtered and the filtrate was concentrated under reduced pressure. The residue was purified by flash column chromatography (DCM/ethyl acetate 4:1) to give 0.47 g (72%) of **3** as a yellow solid. Mp 116–119 °C; IR ν 1364, 1176 (S=O) cm^{-1}; ^1H NMR (500 MHz, $CDCl_3$) (assignments using COSY) δ 8.66 (2H, br d, *J* 8.5 Hz, Nap H-10), 8.30 (2H, dd, *J* 7.5, 1.0 Hz, Nap H-8), 8.27 (2H, d, *J* 8.5 Hz, Nap H-13), 7.64 (2H, dd, *J* 8.5, 7.5 Hz, Nap H-12), 7.57 (2H, dd, *J* 8.5, 7.5 Hz, Nap H-9), 7.25 (2H, br d, *J* 7.5 Hz, Nap H-11), 5.28 (1H, d, *J* 1.0 Hz, CH-7), 5.02 (2H, apparent br t, *J* 4.0 Hz, H-4,6), 4.09–4.12 (1H, m, H-5), 3.96–3.92 (2H, m, H-1,3), 3.90–3.86 (1H, m, H-2), 2.91 (12H, s, NMe_2 dansyl); ^{13}C NMR (75 MHz, $CDCl_3$) 151.9, 132.4, 130.7, 130.6, 129.9, 129.7, 129.6, 123.0, 119.2, 116.0 (Ar–C), 102.7 (C-7), 72.2 (C-4,6), 71.5 (C-5), 67.2 (C-1,3), 60.0 (C-2), 45.4 (NMe_2 dansyl); MS (ES) *m*/*e* $[M+Na]^+$ 679.4. Accurate mass calcd for $C_{31}H_{32}N_2O_{10}S_2Na$: 679.1391; found: 679.1395. Anal. calcd for $C_{31}H_{32}N_2O_{10}S_2 \cdot HCl$: C, 53.71; H, 4.80; N, 4.04. Found: C, 54.26; H, 4.43; N, 3.97%.

4.2.2. 4-O-Dansyl-myo-inositol-1,3,5-orthoformate (5)

Compound **5** was also isolated as a bright yellow solid (0.08 g, 10%). Mp 86–91 °C; IR ν 1358, 1158 (S=O) cm^{-1}; ^1H NMR (500 MHz, DMSO-d_6/D_2O) δ 8.64 (1H, br d, *J* 8.5 Hz, Nap H-10), 8.35 (1H, dd, *J* 7.5, 1.0 Hz, Nap H-8), 8.08 (1H, br d, *J* 8.5 Hz, Nap H-13), 7.75 (1H, dd, *J* 8.5, 7.5 Hz, Nap H-9), 7.70 (1H, dd, *J* 8.5, 7.5 Hz, Nap H-12), 7.33 (1H, br d, *J* 7.5 Hz, Nap H-11), 5.48 (1H, d, *J* 1.0 Hz, CH-7), 4.85 (1H, apparent br td, *J* 4.0, 1.5 Hz, H-4), 4.31(1H, apparent br td, *J* 3.5, 1.5 Hz, H-6), 4.07–4.04 (1H, m, H-5), 3.97–3.94 (2H, m, H-3,2), 3.72–3.69 (1H, m, H-1), 2.86 (6H, s, NMe_2 dansyl); ^{13}C NMR (75 MHz, DMSO-d_6/D_2O) 151.6, 132.0, 130.7, 130.0, 129.1, 128.9, 128.8, 123.7, 118.1, 115.7 (Ar–C), 101.9 (C-7), 74.1 (C-4), 73.5 (C-5), 71.4 (C-3), 69.0 (C-2), 65.6 (C-6), 58.1 (C-1), 44.9 (NMe_2 dansyl); MS (ES) *m*/*e* $[M-H]^-$ 422.5. Accurate mass calcd for $C_{19}H_{20}NO_8S$: 422.0904; found 422.0906. Anal. calcd for $C_{19}H_{21}NO_8S \cdot 0.5H_2O$: C, 52.77; H, 5.13; N, 3.24. Found: C, 52.50; H, 4.44; N, 2.99%.

4.2.3. 4-O-Dabsyl-6-O-dansyl-myo-inositol-1,3,5-orthoformate (6)

Sodium hydride (60%, 0.4 g, 9.9 mmol) was suspended in dry DMF (20 ml) and the mixture was stirred at room temperature under a nitrogen atmosphere. 2-*O*-*tert*-Butyldimethylsilyl-*myo*-inositol-1,3,5-orthoformate[20] **4** (0.3 g, 1.0 mmol) was added to the above solution and the mixture was stirred at room temperature for 10 min. Dabsyl chloride (0.32 g, 1.0 mmol) was added to the above mixture. The mixture was stirred at room temperature under a nitrogen atmosphere for 10 min. Dansyl chloride (0.56 g, 2.1 mmol) was added and the mixture was stirred for a further 24 h. Completion of the reaction was monitored by TLC (DCM/ethyl acetate 3:1), R_f 0.48. The reaction mass was carefully quenched with 20 ml of 0.01 M HCl and then the mixture was diluted with ethyl acetate (100 ml). The layers were separated and the organic layer was washed with water (6×25 ml) followed by 10% $NaHCO_3$ (2×20 ml). The organic layer was dried over anhydrous magnesium sulfate, filtered and the filtrate concentrated under reduced pressure. The residue was purified by flash column chromatography (DCM/ethyl acetate 4:1) to give 0.32 g (45%) of **6** as a dark red solid. Mp 221–225 °C; IR ν 1361, 1183 (S=O) cm^{-1}; ^1H NMR (400 MHz, $CDCl_3$) (assignments made using COSY and NOESY spectra) δ 8.65 (1H, br d, *J* 8.5 Hz, Nap H-10), 8.28 (1H, dd, *J* 7.5, 1.0 Hz, Nap H-8), 8.20 (1H, br d, *J* 8.5 Hz, Nap H-13), 8.02 (2H, dm, *J* 8.5 Hz, Ar H-14/14′), 7.95 (2H, dm, *J* 8.5 Hz, Ar H-15/15′), 7.92 (2H, dm, *J* 9.0 Hz, Ar H-16/16′), 7.64 (1H, dd, *J* 8.5, 7.5 Hz, Nap H-12), 7.56 (1H, dd, *J* 8.5, 7.5 Hz, Nap H-9), 7.23 (1H, br d, *J* 7.5 Hz, Nap H-11), 6.77 (2H, dm, *J* 9.0 Hz, Ar H-17/17′), 5.36 (1H, d, *J* 1.0 Hz, CH-7), 5.19 (1H, apparent td, *J* 4.0, 1.5 Hz, H-4), 5.07 (1H, apparent td, *J* 4.0, 1.5 Hz, H-6), 4.23–4.17 (2H, m, H-3,5), 4.03–3.98 (2H, m, H-1,2), 3.14 (s, 6H, NMe_2 dabsyl), 2.90 (6H, s, NMe_2 dansyl), 2.84 (1H, br d, *J* 12.0 Hz, $OH_{(eq)}$-2); ^{13}C NMR (75 MHz, $CDCl_3$) 156.8, 153.3, 151.9, 143.6, 134.4, 132.4, 130.7 130.6, 129.9, 129.6, 129.1, 126.0, 122.9, 115.9, 111.5 (Ar–C), 102.7 (C-7), 72.0 (C-4), 71.6 (C-6), 71.4 (C-5), 67.1 (C-1,3), 59.9 (C-2), 45.4 (NMe_2 dabsyl), 40.3 (NMe_2 dansyl); MS (ES) *m*/*e* $[M+Na]^+$ 733.5. Accurate mass calcd for $C_{33}H_{34}N_4O_{10}S_2Na$: 733.1609; found: 733.1612.

4.2.4. 4-O-Dabsyl-myo-inositol-1,3,5-orthoformate (7)

Compound **7** was also isolated (0.12 g, 15%) as a dark red solid. Mp 232–235 °C (decomp.); IR ν 1361, 1161 (S=O) cm^{-1}; ^1H NMR (500 MHz, DMSO-d_6/D_2O) δ 8.10 (2H, dm, *J* 8.5 Hz, Ar H-8/8′), 8.00 (2H, dm, *J* 8.5 Hz, Ar H-9/9′), 7.87 (2H, dm, *J* 9.0 Hz, Ar H-10/10′), 6.89 (2H, dm, *J* 9.2 Hz, Ar H-11/11′), 5.53 (1H, d, *J* 1.0 Hz, CH-7), 4.97 (1H, apparent td, *J* 4.0, 1.5 Hz, H-4), 4.32 (1H, apparent td, *J* 4.0, 1.5 Hz, H-6), 4.09–4.12 (1H, m, H-5), 3.89–4.00 (3H, m, H-1,2,3), 3.11 (6H, s, NMe_2 dabsyl); ^{13}C NMR (75 MHz, DMSO-d_6/D_2O) 155.9, 153.4, 142.5 134.0, 129.1, 125.8, 125.5, 122.7, 122.1, 111.6 (Ar–C), 101.9 (C-7), 74.0 (C-4), 73.4 (C-5), 71.4 (C-3), 68.7 (C-2), 65.6 (C-6), 58.1 (C-1), 39.7 (NMe_2 dabsyl); MS (ES) *m*/*e* $[M-H]^-$ 476.5. Accurate mass calcd for $C_{21}H_{22}N_3O_8S$: 476.1122; found: 476.1130.

4.2.5. 4,6-Bisdansyl-myo-inositol (8)

Diester **3** (0.2 g, 0.3 mmol) was treated with 2 ml of 80% trifluoroacetic acid[20] and the mixture was stirred at room temperature for 4 h. The reaction mixture was concentrated under reduced pressure. The residue was diluted with toluene (2×10 ml). The excess toluene was distilled off under reduced pressure and the solid was crystallised from hexane to give 0.14 g (75%) of **8** as a light yellow solid. Mp 138–143 °C (decomp.); IR ν 1339, 1170 (S=O) cm^{-1}; ^1H NMR (500 MHz, $CDCl_3$) δ 8.55 (2H, br d, *J* 8.5 Hz, Nap H-10), 8.27 (2H, d, *J* 8.5 Hz, Nap H-13), 8.22 (2H, dd, *J* 7.5, 1.0 Hz, Nap H-8), 7.52 (2H, dd, *J* 8.5, 7.5 Hz, Nap H-12), 7.48 (2H, dd, *J* 8.5, 7.5 Hz, Nap H-9) 7.18 (2H, d, *J* 7.5 Hz, Nap H-11), 4.83 (2H, apparent t, *J* 9.5 Hz, H-4,6), 4.10 (1H, t, *J* 2.5 Hz, H-2), 3.58–3.64 (3H, m, H-1,5,3), 2.89 (12H, s, NMe_2 dansyl); ^{13}C NMR (75 MHz, $CDCl_3$) 151.2, 131.9, 131.6, 130.2, 130.0, 129.5, 128.7, 123.2, 119.6, 115.6 (Ar-C), 84.3 (C-4,6), 71.7 (C-5), 70.2 (C-1,3), 69.6 (C-2), 45.5 (NMe_2 dansyl). MS (ES) *m*/*e* $[M-H]^-$ 645.7. Accurate mass calcd for $C_{30}H_{34}N_2O_{10}S_2Na$: 669.1547; found: 669.1544. Anal. calcd for $C_{30}H_{34}N_2O_{10}S_2 \cdot CF_3COOH$: C, 50.52; H, 4.64; N, 3.68. Found: C, 51.03; H, 4.86; N, 3.35%.

4.2.6. 4-Dabsyl-6-dansyl-myo-inositol (9)

Diester **6** (0.1 g, 0.14 mmol) was treated with 1 ml of 80% trifluoroacetic acid[20] and the mixture was stirred at room temperature for 4 h. The reaction mixture was basified with 2 ml of triethylamine and concentrated under reduced pressure. The residue was diluted with toluene (2×5 ml). The excess toluene was distilled off under reduced pressure and the residue was purified by column chromatography (EtOAc/CH_2Cl_2 50:50) to give 0.03 g (32%) of **9** as an orange oil. IR ν 1350, 1183 (S=O) cm^{-1}; ^1H NMR (400 MHz, CD_3OD)

δ 8.57 (1H, br d, *J* 8.6 Hz, Nap H-10), 8.23 (1H, dd, *J* 7.3, 1.1 Hz, Nap H-13), 8.19 (1H, d, *J* 8.7 Hz, Nap H-8), 8.03 (2H, dm, *J* 8.7 Hz Ar H-14/14′), 7.88 (4H, dm, *J* 8.9 Hz, Ar H-15/15′ and 16/16′) 7.59 (1H, dd, *J* 8.5, 7.4 Hz, Nap H-9), 7.52 (1H, dd, *J* 8.5, 7.7 Hz, Nap H-12), 7.24 (1H, d, *J* 7.6 Hz, Nap H-11), 6.78 (2H, dm, *J* 9.2 Hz, Ar H-17/17′), 5.09 (1H, apparent t, *J* 9.8 Hz, H-4), 4.87–4.81 (2H, m, H-5,6), 3.95 (1H, t, *J* 2.6 Hz, H-2), 4.01–3.99 (2H, m, H-1,3), 3.14 (6H, s, NMe_2 dabsyl), 2.90 (6H, s, NMe_2 dansyl); ^{13}C NMR (75 MHz, CD_3OD) 157.3, 155.0, 153.0, 144.9, 139.0, 135.7, 132.1, 131.2, 130.4, 130.2, 126.8, 123.1, 112.7 (Ar–C), 86.5 (C-4), 83.6 (C-6), 78.4 (C-5), 73.1 (C-2), 71.6 (C-3), 71.6 (C-1), 45.8 (NMe_2 dabsyl), 40.4 (NMe_2 dansyl); MS (ES) *m*/*e* $[M+Na]^+$ 723.8. Accurate mass calcd for $C_{32}H_{36}N_4O_{10}S_2Na$: 723.1765; found: 723.1755.

*4.2.7. 4-O-Dansyl-myo-inositol (**10**)*

Compound **10** was also isolated (0.01 g, 12%) as a yellow oil. ^1H NMR (300 MHz, CD_3OD) δ 8.64 (1H, br d, *J* 8.2 Hz, Nap H-10), 8.51 (1H, d, *J* 8.7 Hz, Nap H-8), 8.33 (1H, d, *J* 7.3 Hz, Nap H-13), 7.76–7.64 (3H, m, *J* 8.5, 7.5 Hz, Nap H-9,11,12), 4.84 (1H, apparent t, *J* 9.6 Hz, H-4), 3.87 (1H, t, *J* 2.5 Hz, H-2), 3.61 (1H, apparent t, *J* 9.5 Hz, H-5), 3.51 (1H, dd, *J* 9.8, 2.6 Hz, Nap H-3), 3.24 (1H, apparent t, *J* 9.4 Hz, H-6), 3.08–3.14 (1H, m, H-1), 3.15 (6H, s, NMe_2 dansyl);^{13}C NMR (75 MHz, CD_3OD) 151.4, 136.7, 131.3, 130.7, 129.2, 129.1, 128.8, 125.9, 125.3, 118.3 (Ar–C), 87.9 (C-4), 74.3 (C-2), 74.2 (C-5), 74.0 (C-3), 72.8 (C-6), 71.1 (C-1), 46.7 (NMe_2 dansyl); Fluorescence λ_{max} (water) 590 nm; MS (ES) *m*/*e* $[M+H]^+$ 414.1. Accurate mass calcd for $C_{18}H_{24}NO_8S$: 414.1217; found: 414.1210.

Acknowledgements

Overseas Research Scholarship and University of Manchester award to M.K. Research funded in part by the The Great Socialist People's Libyan Arab Jamahiriya (The Secretariat of Higher Education, Professor Akeel Hussain Akeel).

References and notes

1. Bichenkova, E. V.; Savage, H. E.; Sardarian, A. R.; Douglas, K. T. *Biochem. Biophys. Res. Commun.* **2005**, *332*, 956–964.
2. Bichenkova, E. V.; Sardarian, A.; Savage, H. E.; Rogert, C.; Douglas, K. T. *Assay Drug Dev. Technol.* **2005**, *3*, 39–46.
3. Bichenkova, E. V.; Yu, X.; Bhadra, P.; Heissigerova, H.; Pope, S. J. A.; Coe, B. J.; Faulkner, S.; Douglas, K. T. *Inorg. Chem.* **2005**, *44*, 4112–4114.
4. Lakowicz, J. *Principles of Fluorescence Spectroscopy*, 2nd ed.; Plenum: New York, NY, 1999.
5. Levi, J.; Cheng, Z.; Gheysens, O.; Patel, M.; Chan, C. T.; Wang, Y.; Namavari, M.; Gambhir, S. S. *Bioconjugate Chem.* **2007**, *18*, 628–634.
6. Cheng, Z.; Levi, J.; Xiong, Z.; Gheysens, O.; Keren, S.; Chen, X.; Gambhir, S. S. *Bioconjugate Chem.* **2006**, *17*, 662–669.
7. Payre, N.; Cottaz, S.; Driguez, H. *Angew. Chem., Int. Ed. Engl.* **1995**, *34*, 1239–1241.
8. Oh, K.-B.; Matsuoka, H. *Int. J. Food Microbiol.* **2002**, *76*, 47–53.
9. Kadirvel, M.; Bichenkova, E. V.; D'Emanuele, A.; Freeman, S. *Chem. Lett.* **2006**, *35*, 868–869.
10. Wuts, P. G. M.; Greene, T. W. *Greene's Protective Groups in Organic Synthesis*, 4th ed.; John Wiley and Sons: New Jersey, NJ, 2006; 348–350.
11. Murali, C.; Shashidhar, M. S.; Gopinath, C. S. *Tetrahedron* **2007**, *63*, 4149–4155.
12. Gilbert, I. H.; Holmes, A. B. *Tetrahedron Lett.* **1990**, *31*, 2633–2634.
13. Yeh, S.-M.; Lee, G. H.; Wang, Y.; Luh, T.-Y. *J. Org. Chem.* **1997**, *62*, 8315–8318.
14. Johansson, M. K.; Cook, R. M. *Chem.—Eur. J.* **2003**, *9*, 3466–3471.
15. Gruber, B. A.; Leonard, N. J. *Proc. Natl. Acad. Sci. U.S.A.* **1975**, *72*, 3966–3969.
16. Marme, N.; Knemeyer, J.-P.; Sauer, M.; Wolfrum, J. *Bioconjugate Chem.* **2003**, *14*, 1133–1139.
17. Tzeng, M. C. *Anal. Biochem.* **1983**, *128*, 412–414.
18. Parkinson, D.; Redshaw, J. D. *Anal. Biochem.* **1984**, *141*, 121–126.
19. Lee, H. W.; Kishi, Y. *J. Org. Chem.* **1985**, *50*, 4402–4404.
20. Angyal, S. J. *Carbohydr. Res.* **2000**, *325*, 313–320.
21. Sureshan, K. M.; Shashidhar, M. S.; Praveen, T.; Gonnade, R. G.; Bhadbhade, M. M. *Carbohydr. Res.* **2002**, *337*, 2399–2410.
22. Weber, G. *Biochem. J.* **1952**, *51*, 155–167.
23. Johansson, M. K.; Fidder, H.; Dick, D.; Cook, R. M. *J. Am. Chem. Soc.* **2002**, *124*, 6950–6956.
24. Bravo, J.; Mendicuti, F.; Mattice, W. L. *J. Polym. Sci., Part B: Polym. Phys.* **1994**, *32*, 1511–1519.
25. SYBYL 7.3 (2006), Tripos Associates, 1699 South Hanley Road, Suite 303, St. Louis, MO, 63144-2917.
26. Clark, M.; Cramer, R. D., III; Van Opdenbosch, N. *J. Comput. Chem.* **1989**, *10*, 982–1012.